

# Reconsidering Himalayan river anticlines

David R. Montgomery\*, Drew B. Stolar

*Quaternary Research Center and Department of Earth and Space Sciences, University of Washington, Seattle, WA 98195, USA*

Received 2 July 2004; received in revised form 27 August 2005; accepted 27 August 2005

Available online 5 June 2006

## Abstract

The observation that major Himalayan rivers flow parallel to and down the axis of anticlines oriented transverse to the primary structural grain of the range has puzzled geomorphologists for decades. Although there is a general consensus that the courses of trans-Himalayan rivers predate the Himalayan orogeny, the close association of rivers and structural highs would not be expected to result from the superposition of rivers onto pre-existing structures. Moreover, in the past several decades structural studies have shown that the development of river anticlines represents the most recent phase of deformation in the range. It is proposed that Himalayan river anticlines are the consequence of focused rock uplift in response to significant differences between net erosion along major rivers and surrounding regions. This hypothesis is supported by large gradients in observed and predicted erosion rates across major Himalayan rivers and by results from an isostasy-driven model, which requires relatively low flexural rigidities to match the wavelength of Himalayan river anticlines. Whether the amplitude of these structures is due to isostasy or also reflects active crustal channeling is not well-constrained, but given the uncertainty in the flexural rigidity and in the local and far-field erosion rates, both possibilities remain viable explanations. Given the observed correlation between the Arun River anticline and local rainfall maxima, it is proposed that Himalayan river anticlines are the expression of a relatively fine-scale linkage between tectonics, erosion and climate superimposed on the broader and older canvas of the Himalayan orogeny. Finally, it is suggested that the development of river anticlines represents one example along a continuum of features arising from different degrees of erosion-structure coupling in active orogens.

© 2006 Elsevier B.V. All rights reserved.

*Keywords:* Bedrock erosion; River anticline; River incision; Himalayan rivers; Arun

## 1. Introduction

Classical explanations for spatial relations between rivers and geologic structure involve rivers passively following structural lows, faults or zones of weakness, or maintaining their grade across developing structures such as growing anticlines. Cases where rivers flow along structural highs are known as river anticlines and, as noted by Oberlander (1985), are common along

Himalayan rivers. Wager (1937) originally noted that the Arun River flows along synclines in Tibet and then drops through the Himalaya in a gorge along an anticline carved into hard, deeply-exhumed gneiss and suggested that the most recent phase of Himalayan uplift was due to isostatic response to incision of deep river valleys.

The amplitude and wavelength of anticlines along the Indus and Arun rivers are apparent on maps and cross-sections reported in previous work. Cross-sections across the Indus River (DiPietro et al., 1999) show the river centered on the crest of a 10-km amplitude anticline with a wavelength of 50 to 60 km. Meier and

\* Corresponding author.

E-mail address: [dave@ess.washington.edu](mailto:dave@ess.washington.edu) (D.R. Montgomery).

Hiltner's (1993) map of the distribution of metamorphic units and associated cross-section through the Arun Tectonic Window shows an anticline with an amplitude of about 10 km and a wavelength of about 30 km. Oberlander (1985) also estimated the amplitude of the Arun River Anticline as 10 km. The mapping of Schelling (1992) revealed that the Arun River Anticline is actually one of the several in the region and that the adjacent drainage divides coincide with north–south trending synclines. Also, the area of deeply exhumed rocks along the gorge of the Tsangpo River in the eastern Himalayan syntaxis is a roughly 60 to 80 km-wide antiform (Burg et al., 1997). Hence, it appears that local antiformal structural highs along major Himalayan rivers have wavelengths of 30 to 80 km.

Recent work on linkages between spatial patterns in erosion rates and rock uplift suggests that the geography of erosion may in some circumstances influence, or even control the evolution of geological structures. Zeitler et al. (2001), for example, proposed that focused bedrock river incision can concentrate rock uplift and exhumation, which in turn advects hot weak rock toward the surface and results in a positive feedback and development of a deeply-exhumed antiformal metamorphic massif. Although the idea that progressive river incision into the bedrock could generate river anticlines was rejected by Oberlander (1985) in his interpretation of the origin of Himalayan river anticlines, classical ideas do not provide satisfying explanations for these features. Most workers view the crust as rigid, which implies that the incision of short-wavelength river valleys would exert little influence on crustal deformation. However, Simpson (2004) recently simulated the development of anticlines transverse to rivers using a landscape evolution model and found that “river incision can have a major influence on deformation of the surrounding crust if incision occurs at the same time that the crust is deforming plastically in response to regional compression.” In this paper prior work on river anticlines is reviewed and the conditions are explored under which one would expect the potential for rivers to influence the growth of local geological structures through sustained differences in bedrock erosion.

## 2. Previous work

Attempts to explain and systematize genetic relationships between rivers and geologic structure can be traced back to Powell's (1875) classification of valleys into antecedent and consequent types. Since Powell's recognition that valleys could either pre-date (antecedent) or post-date (consequent) the development of the

geological structures over which they flow, relationships between rivers and geological structure have been actively investigated (e.g., Tucker and Slingerland, 1994; Norris and Cooper, 1997; Pavlis et al., 1997; Burbank et al., 1999). The case of rivers occupying structural lows or the axis of synclines requires no special explanation, particularly for alluvial rivers in rift zones or those trapped in structural depressions. In contrast, several general explanations have been developed for the less intuitive case of rivers that flow across or along structural highs, particularly rivers flowing along the crest of anticlines.

The most common explanation for the orientation of rivers flowing transverse to geologic structure is that of drainage superposition, in which the course of the river across the geological structure was inherited. Antecedent rivers also may cross geological structures where rivers are competent enough to cut either across structures exposed by progressive bedrock erosion or through rising structures (e.g., Burbank et al., 1999). However, no particular relation is expected between structure and drainage in both the case where a river maintains its course while structures rise around it, and the case where the river's course is superimposed on underlying rocks as the river cuts down into them.

Rivers that bisect the Zagros Mountains are the classic example of drainage superposition (Oberlander, 1965), and the major drainages of the Himalaya, which generally flow transverse to the orientation of the range, are also thought to have been formed by antecedent rivers that flowed across the edge of the rising Tibetan Plateau at the onset of and during the Himalayan orogeny (Wager, 1937; Gansser, 1964; Oberlander, 1985). Alvarez (1999) and Simpson (2004) describe additional examples of relationships between transverse rivers and structure highs in the central Apennine fold-and-thrust belt, the Pyrenees, the Swiss and French Alps, and the central Andes. After noting an “uncanny homing instinct of larger streams” to find and flow through anticlines despite the presence of proximal structural lows that the rivers appeared to avoid, Oberlander (1985) offered an elaborate model for how a combination of drainage antecedence and superposition could lead to rivers flowing through structural highs in rocks with strong contrasts in erodibility. Alvarez (1999), however, showed that the particular stratigraphic sequence invoked by Oberlander as required for such a scenario in the Zagros Mountains was lacking in the case of the Apennines, despite the development of similar structures. Moreover, in the general case of drainage superposition there should not be any particular relation between river courses and the geological

structures onto which they were superimposed. Neither should there be any particular relation for pre-existing rivers that maintained their grade across developing or active structures.

In contrast, differential erosion should result in close association between rivers and structural highs where weak rocks become exposed at the surface and trap rivers into flowing along the core of an eroding anticline. In such cases, the deformation leading to the development of the geological structures pre-dates the establishment of the drainage system. The Appalachian mountains contain numerous well-known examples of rivers flowing in such structurally controlled settings, as taught in introductory geomorphology classes.

River anticlines associated with salt dome structures along the Colorado River near the Colorado–Utah border present a more unusual example of “salt tectonics” driven by river incision (Harrison, 1927). There, a series of saline anticlines, or salt domes have up to 300 m of structural relief and are centered on the river. Harrison (1927) explained the development of these features as due to isostatic response to differential erosion along the river. In his view, as the river cut its canyon the progressive development of differential loading between the canyon walls and the valley bottom triggered the buoyancy-driven rise of underlying salt along the river — the locus of focused erosion.

The river anticlines along the Colorado River in the central Grand Canyon provide another unusual example of geological structures formed in response to river incision (Huntoon and Elston, 1979). At the base of the Grand Canyon, strata of the Cambrian Mauv Limestone and the underlying Cambrian Bright Angel Shale are locally warped into river-parallel anticlines with 5–10 m amplitudes and 200–400 m wavelengths, and which follow the course of the river around bends. Huntoon and Elston (1979) showed that these features were likely an unloading phenomenon due to the stress gradient induced by the juxtaposition of the 650-m-high canyon walls and the unloaded valley floor.

Himalayan rivers provide another example of a peculiar, and unexplained, relationship between river courses and geologic structure. Major Himalayan rivers run transverse to the primary geologic structures across the range, from the edge of the Tibetan Plateau across the primary thrust faults that parallel the general trend of the range itself. In contrast to this general trend, Bordet (1955) noted that the axes of the Arun and Karnali rivers in the eastern Himalaya followed “transanticlines” that crossed the primary structural trend in the range. While there appears to be a broad consensus that trans-

Himalayan rivers are antecedent, Meier and Hiltner (1993) showed that the deformation associated with the growth of the river-parallel anticline along the Arun River is the youngest regional deformation and that it post-dates both metamorphism and development of collision-related structures. This precludes the possibility that the river anticline is simply part of the inherited geologic structure beneath an antecedent river, and along which the modern river coincidentally flows. According to Krishnaswamy (1981) many of the major rivers of the central Himalaya follow range-transverse folds that are the result of the youngest deformation in the range. Through examination of geological maps, Oberlander (1985) found that in addition to the Arun and Karnali rivers, the Tista, Kali Gandaki, and Sutlej rivers all follow anticlines oriented transverse to the primary structural grain of the range. The Indus and Tsangpo rivers also flow through deeply exhumed structural highs where they turn abruptly and flow through steep gorges to cross the Himalaya (Burg et al., 1997; DiPietro et al., 1999). If the major trans-Himalayan rivers are antecedent, as generally agreed, then why do they coincide with the youngest deformation in the range — deformation transverse to the primary structural grain?

Traditional explanations do not satisfactorily explain the development of Himalayan river anticlines. The high-grade metamorphic rocks exposed in the core of these anticlines are not relatively weak, as would be required to explain them as a simple product of differential erosion, like in the Appalachians. Anticlines with amplitudes larger than the relief of the valley cannot be generated by stress release, as seen in how the river valley dwarfs the small river anticlines along the Colorado River. In addition, because the anticline along the Arun River is younger than both the regional metamorphism and collision-related structures, the river could not have been simply superimposed on an underlying structure. Oberlander (1985) nonetheless favored drainage superposition as the most likely explanation for why Himalayan rivers are perched on top of large folds, although he recognized that the strong association of the river with these structures presented a fundamental problem to this interpretation.

[U]nless we accept the presence of gigantic “river anticlines” in the Himalaya, produced by off-loading as canyons are cut, we have a problem of reconciling so-called “antecedent” streams, that should conspicuously disregard structure, with an apparent stream preference for a particular structural environment. (Oberlander, 1985, p. 159)

Wager's original idea that the great height of the Himalayan peaks was due to local isostatic response to unloading would require a low flexural rigidity in a region with substantial crustal thickness (Montgomery, 1994). Despite the lack of satisfying answers as to how Himalayan river anticlines formed, the problem virtually lay dormant until Zeitler et al. (2001) proposed that rapid river incision into bedrock contributed to the formation of active crustal aneurysms in the Himalayan syntaxes. Finlayson et al. (2002) subsequently suggested that non-uniform bedrock erosion might be responsible for the spatial association of zones of predicted rapid river incision and both syntaxial metamorphic massifs and Himalayan river anticlines.

Exploring the scenario dismissed by Oberlander, Simpson (2004) addressed the potential for anticline formation in response to river incision through numerical experiments using a coupled mechanical-surface process model. Specifically, he coupled a thin elastic-plastic plate with a surface process model that included both hillslope diffusion and river incision. He assumed a relatively stiff crust and considered three combinations of boundary conditions: (i) localized river incision during horizontal compression; (ii) flexural response to river incision in the absence of regional compression; and (iii) regional compressive deformation without river incision. He found that the response to river incision in the absence of compression was minor, amounting to structurally negligible amounts of rebound in the specific scenario he reported, and that incision under regional compression produced doubly plunging transverse anticlines with structural culminations that coincided with the location crossed by the river. Based on this analysis, he concluded that "whether rivers exert an influence on local deformation depends critically on the timing between river incision and regional deformation" (Simpson, 2004).

Here further consideration is given to the question of whether spatial variability in bedrock erosion could, during progressive unroofing over geologic time, lead to the development of river anticlines such as those reported along major Himalayan rivers.

### 3. Study area

The Arun River is the focus because it is the classic example of a river anticline, and because of the availability of regional geologic mapping that depicts the axes of synclines and anticlines transverse to the range. Schelling (1992) mapped the geology of eastern Nepal from the Kathmandu Valley to the Sikkhim border and from the High Himalaya to the Ganges Plain (Fig.

1A). The area has the well known primary structural and stratigraphic grain found throughout much of the range — proceeding south to north, the alluvial plain of the Ganges basin, the Main Frontal Thrust (MFT), the Sub-Himalayan sequence of sedimentary rocks, the Main Boundary Thrust (MBT), the Lesser Himalayan Series rocks, the Main Central Thrust (MCT), and the Higher Himalayan crystalline and Tibetan rocks. Although the primary structural grain parallels the strike of the range, structural windows including the Arun Tectonic Window (Meier and Hiltner, 1993) expose rocks below the MCT, which is deformed in a series of anticlines and synclines, the axes of which roughly parallel major rivers and drainage divides, respectively.

Annual rainfall in the region exhibits a double-band pattern typical of the Central and Eastern Himalaya (Fig. 1B; Anders et al., 2006). Superimposed on the decrease in rainfall with increasing elevation are maxima on the lowest flanks of the range and on slopes just south of the major peaks. This northern band is particularly pronounced in major river valleys like the Arun, which act as conduits for northward transport of monsoonal precipitation (Thiede et al., 2004; Anders et al., 2006). The result is that local precipitation within the gorge of the Arun River is several times greater than in surrounding areas.

### 4. Model

Calculating landscape-scale erosion rates in steep terrain typically involves predicting long-term erosion rates set by rivers as a function of discharge, slope, and bedrock erodibility. We used the unit stream power ( $\Omega$ ) model recently proposed by Finnegan et al. (2005) that incorporates local changes in channel width via

$$\Omega = \rho g Q S / W = k Q^{5/8} S^{19/16} \quad (1)$$

where  $\rho$  is the density of water,  $g$  is gravitational acceleration,  $Q$  is fluvial discharge,  $S$  is river slope,  $W$  is the channel width, and  $k$  is a proportionality constant. The discharge  $Q$  is estimated from a 4-year average of precipitation rates derived from Tropical Rainfall Monitoring Mission (TRMM) radar data (Anders et al., 2006). The SRTM 3 arc-second digital elevation model (nominal 90-m grid resolution) is utilized and the channel network is defined as those grid cells with contributing areas greater than 10 km<sup>2</sup> to restrict the analysis to main stem channels and large tributaries. Doing so avoided application of Eq. (1) to debris-flow-dominated headwater channels, hillslopes, and steep valley walls. Standard pit-filling techniques on the Arun River resulted in long reaches of flat channel. These

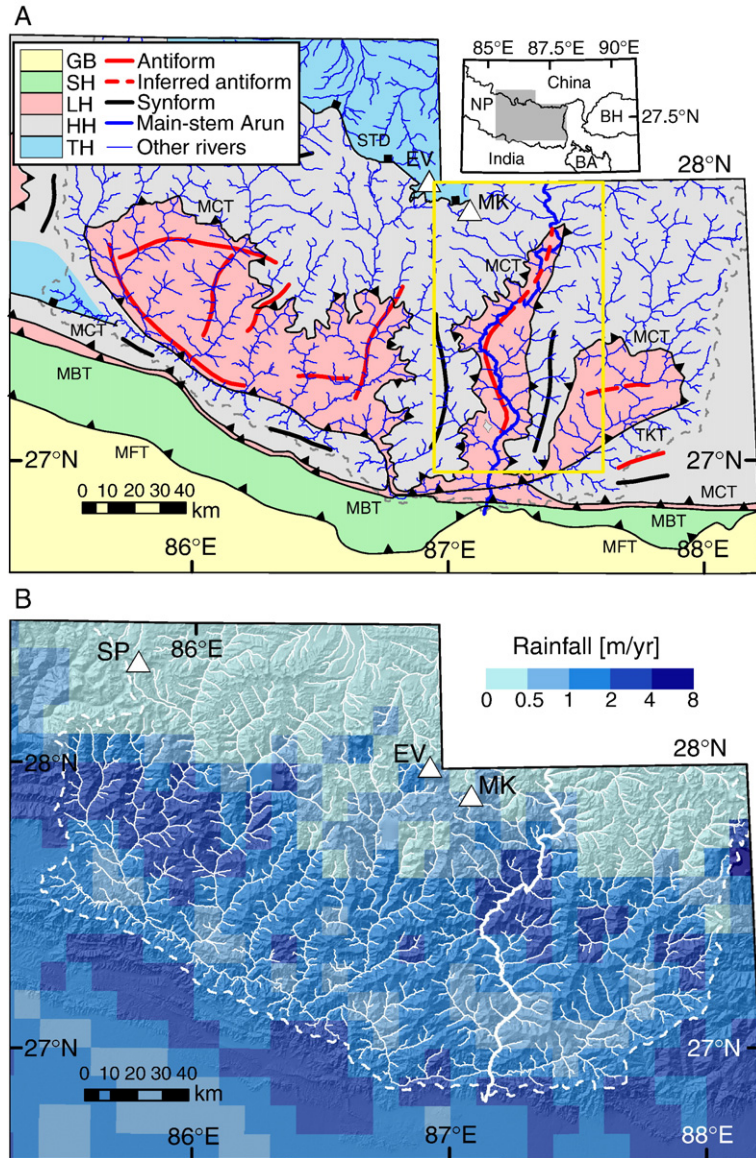


Fig. 1. (A) Geologic map of eastern Nepal (after Schelling, 1992), and (B) precipitation map draped on shaded DEM of the area. Triangles show locations of major peaks (EV = Everest; MK = Makalu; SP = Shisha Pangma). Inset shows location of study area (NP = Nepal; BH = Bhutan; BA = Bangladesh). Stratigraphic abbreviations are as follows: GB = Ganges Basin, SH = Sub-Himalaya; LH = Lesser Himalaya; HH = High Himalaya; TH = Tibetan Himalaya. Structural abbreviations are: MFT = main frontal thrust; MBT = main boundary thrust; MCT = main central detachment; STD = South Tibetan detachment; TKT = Tamar Kola Thrust.

sections were removed, and channel slopes were calculated at the remaining points by linear regression of the elevation profile over 1-km and 5-km length scales. Because information is lacking on the spatial distribution of  $k$  an erosion index given by

$$EI = \Omega/k = Q^{5/8} S^{19/16} \quad (2)$$

was used to generate a predicted pattern of spatial variability in erosion rates.

A simple model was also used to examine the hypothesis that isostatic rebound from bedrock erosion concentrated along a river valley could drive the development of an anticlinal pattern of rock uplift centered along the river. Specifically, we calculate the isostatic response to differential erosion between a uniform erosion rate in the far field and a higher rate within a river valley of width  $L$ . The net difference between near-field and far-field erosion

( $\Delta E$ ) is assumed not to influence the flexural rigidity. In such a scenario, both the valley width and the flexural rigidity of the continental crust influence the length scale across which differential rock uplift will be spread in response to concentrated bedrock river incision. Simply put, larger valleys produce longer wavelength responses than smaller valleys, and weaker crust produces both narrower wavelength and higher amplitude response.

The flexural rigidity of the crust ( $D$ ) depends on its effective elastic thickness ( $T$ ) and is given by

$$D = ET^3/12(1-\nu^2), \quad (3)$$

where  $E$  is the elastic modulus ( $E=8.35 \times 10^{10}$  Nm<sup>-2</sup>) and  $\nu$  is Poisson's ratio ( $\nu=0.25$ ). Thin or mechanically weak crust will concentrate isostatic rock uplift near the area of greatest erosion, whereas thick or strong crust will disperse the response across much broader areas. In addition, substantial crustal strength will reduce the magnitude of isostatically-induced rock uplift to less than expected for the case of Airy isostasy that replaces roughly five-sixths of the rock stripped by erosion.

The solution for the isostatic response,  $w(x)$ , as a function of distance  $x$  from the valley center can be separated into expressions valid inside and outside the river valley, respectively (Hetenyi, 1946):

$$0 < x < L/2 : w(x) = \alpha w_o \left[ e^{-(\frac{L-x}{2})/\alpha} \cos\left(\frac{\frac{L-x}{2}}{\alpha}\right) + e^{-(\frac{L+x}{2})/\alpha} \cos\left(\frac{\frac{L+x}{2}}{\alpha}\right) - 2 \right], \quad (4a)$$

$$x > L/2 : w(x) = \alpha w_o \left[ e^{-(\frac{L+x}{2})/\alpha} \cos\left(\frac{\frac{L+x}{2}}{\alpha}\right) - e^{-(x-\frac{L}{2})/\alpha} \cos\left(\frac{x-\frac{L}{2}}{\alpha}\right) \right], \quad (4b)$$

where  $\alpha$  is the flexural parameter

$$\alpha = (4D/\rho_m g)^{1/4}, \quad (5)$$

and  $w_o$  is the isostatic response at the valley center due to a point load

$$w_o = \rho_c g \Delta E \alpha^3 / 8D. \quad (6)$$

The wavelength ( $\lambda$ ) of the isostatic response can be derived from Eq. (4b), and is given by

$$\lambda = 2\alpha \tan^{-1} \left( \frac{1 - e^{L/\alpha}}{1 + e^{L/\alpha}} \cot\left(\frac{L}{2\alpha}\right) \right). \quad (7)$$

Similarly, the maximum amplitude of the response, which occurs at the valley center ( $x=0$ ), can be extracted from Eq. (4a):

$$w_{\max} = \Delta E \frac{\rho_c}{\rho_m} \left[ 1 - e^{-\frac{L}{2\alpha}} \cos\left(\frac{L}{2\alpha}\right) \right]. \quad (8)$$

Non-dimensionalization of Eq. (8) yields the amplitude of the isostatic response as a proportion of the total amount of material eroded:

$$w_{\max}^* = \frac{w_{\max}}{\Delta E} = \frac{\rho_c}{\rho_m} \left[ 1 - e^{-\frac{L}{2\alpha}} \cos\left(\frac{L}{2\alpha}\right) \right]. \quad (9)$$

Given independent knowledge of the differences in net erosion ( $\Delta E$ ), Eq. (9) can be used to estimate the amplitude of the resulting geological structure in relation to the thickness of the material removed.

## 5. Model results

Predicted values of the erosion index are greatest along the Arun River where it flows through its gorge in the northern half of the modeled area (Fig. 2). The axis of the anticline in the Arun Tectonic Window tracks the zone of high predicted erosion potential in the northern part of the area (through the gorge) where there is a more than two order of magnitude difference in the erosion index between the main stem and the upper reaches of the surrounding tributaries. In particular, the erosion index progressively increases down tributaries to the gorge across a roughly 10–20 km wide zone of high erosion potential centered on the gorge of the Arun River. However, the zone of high contemporary erosion potential only extends about 10 km south of 27.5° N.

The wavelength of flexurally-mediated isostatic response predicted by Eq. (7), and therefore the wavelength of any anticline produced by such response, is essentially independent of valley width for  $D > 10^{21}$  N m, but becomes increasingly sensitive to variations in valley width for  $D < 10^{21}$  N m (Fig. 3). For valley widths of 10 to 20 km, a reasonable range for large Himalayan valleys and roughly the scale of the zone of high EI predicted along the Arun River, Eq. (7) predicts that the

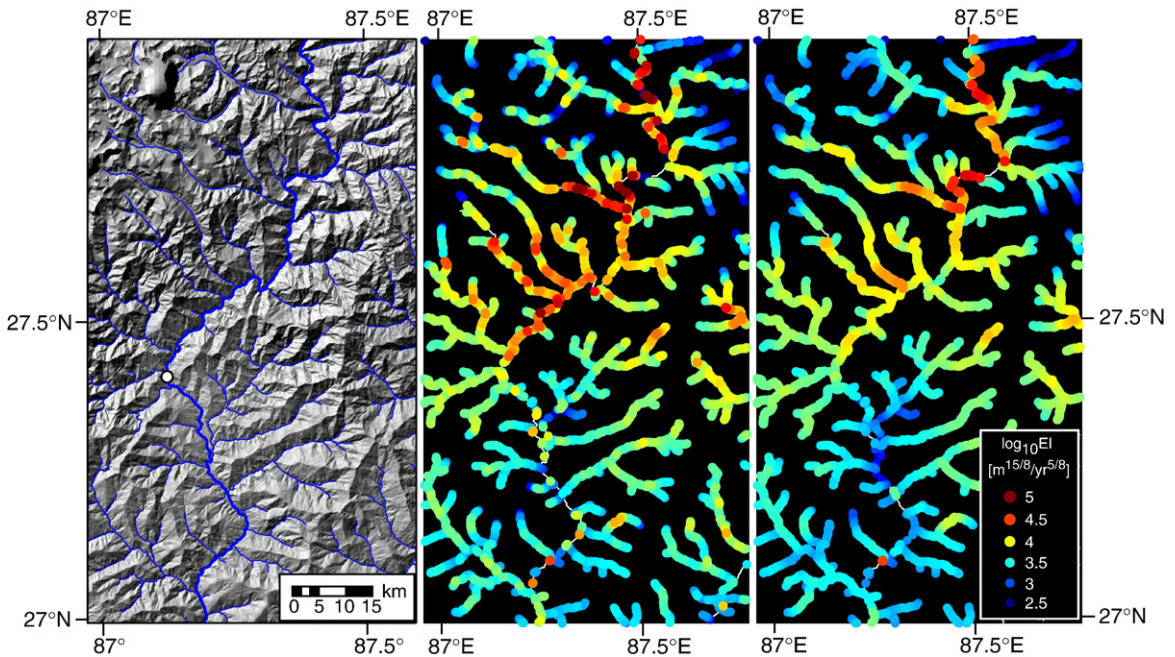


Fig. 2. (A) Shaded relief map of the Arun gorge area based on the 3 arc-second SRTM DEM; (B) Erosion index (EI) map based on 1 km slope averaging within channel network defined by grid cells with drainage area >10 km<sup>2</sup>; (C) comparable EI map based on 5 km slope averaging.

zone of rock uplift in response to localized river incision will have a wavelength of about 50 km to 90 km for flexural rigidities of 10<sup>20</sup> to 10<sup>21</sup> N m. For the same range in valley width and rigidity, the predicted amplitude of the isostatic response, expressed as a fraction of total amount of material removed, ranges from 0.2 to almost 0.7 (Fig. 4). However, as is apparent from Figs. 3 and 4, the full range of potential linkages

between focused bedrock erosion and structural response manifest across just two orders of magnitude in flexural rigidity (from 10<sup>20</sup> to 10<sup>22</sup> N m), making independent knowledge of this often poorly constrained parameter of central importance to understanding the role of isostatic response in the development of Himalayan river anticlines.

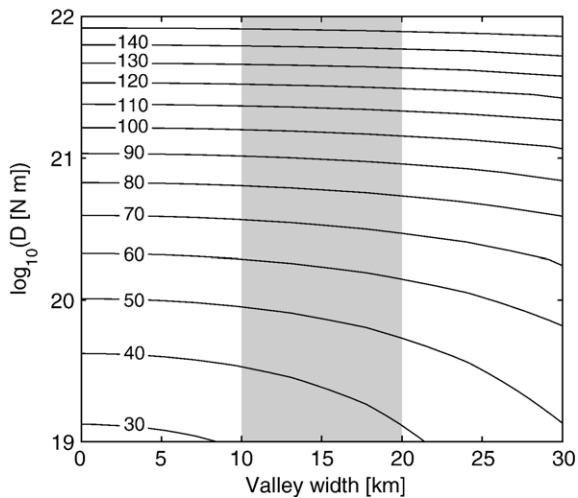


Fig. 3. Wavelength of flexural isostatic rebound (contours in units of km) as a function of valley width (km) and flexural rigidity (N m), as predicted by Eq. (7).

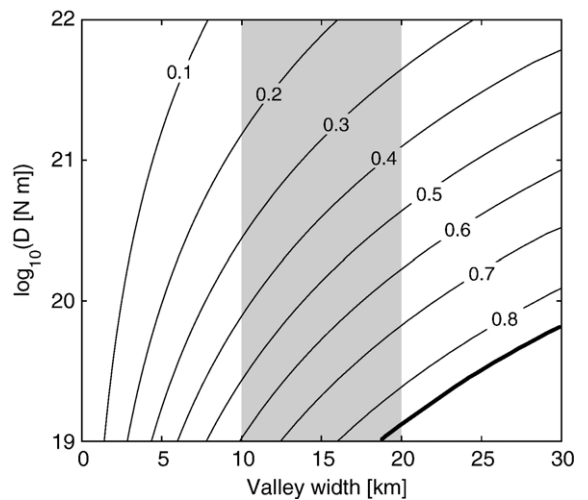


Fig. 4. Non-dimensional magnitude of flexural rebound (contours express rebound as a proportion of the thickness of material eroded) as a function of valley width (km) and flexural rigidity (N m), as predicted by Eq. (9).

## 6. Discussion

In order for erosion to cause differential isostatic rock uplift, and thereby contribute to forming river anticlines, erosion of the main river valley must outpace the background rock uplift rate and the erosion rate in surrounding areas. If the latter condition was not true, isostatic rebound would simply result in uniform rock uplift. In the steep topography of the Himalaya, and in particular along the steep river gorges associated with river anticlines, the rate of bedrock river incision is thought to set the lowering rate of the surrounding slopes (e.g., Burbank et al., 1996; Montgomery, 2001). Hence, rates of river incision should set long-term bedrock erosion rates along major river valleys. Previous modeling of erosion potential using coarser-resolution DEMs – whether cast either in terms of estimated stream power, unit stream power, or basal shear stress – shows the Arun, Indus, Sutlej, and Tsangpo rivers as having substantially greater local erosion potential than the Himalaya in general (Finlayson et al., 2002), as also suggested by our finer-scale model for the gorge of the Arun River.

Comparison of whole-basin erosion rates to local river incision rates supports the prediction of greater-than-average local river incision along portions of major Himalayan rivers (Table 1). Whole-basin erosion rates compiled by Lavé and Avouac (2001) for eleven Himalayan drainage basins range from 0.4 to 2.5 mm year<sup>-1</sup>. In particular, they reported denudation rates of 0.4 to 0.6 mm year<sup>-1</sup> for the Arun River basin based on suspended sediment yields. Schumm (1963) reported an average denudation rate of 1 mm year<sup>-1</sup> for the Kosi River (into which the Arun flows) based on previously reported reservoir infilling rates. Based on measured sediment loads Das (1968) reported erosion rates of 0.5, 1.0, and 1.4 mm year<sup>-1</sup>, respectively, for the Arun, Sapta Kosi, and Sun rivers, and 2.6 mm year<sup>-1</sup> for the more anthropogenically disturbed Tamar River. In contrast, Lavé and Avouac (2001) reported river incision rates of 1 to 8 mm year<sup>-1</sup> along the Arun River based on <sup>14</sup>C dated terrace elevations, and also presented calibrated models of river incision that predicted local incision of 4–8 mm year<sup>-1</sup> along the Arun and other rivers in the High Himalaya.

Local river incision rates reported for the other major Himalayan rivers also are up to an order of

Table 1  
Himalayan erosion rates

Aerial extent	Rate (mm year <sup>-1</sup> )	Method	Source
<i>Whole range</i>			
High Himalaya	1.0	Post 20 Ma exhumation	Einsele et al. (1996)
Himalayan basins	2.1–2.9	Geochemical mass-balance	Galy and France-Lanord (2001)
<i>Whole basins and local far-field erosion rates</i>			
Himalayan basins	0.4–2.5	Suspended sediment load	Lavé and Avouac (2001)
Arun River	0.4–0.6	Suspended sediment load	Lavé and Avouac (2001)
Arun River	0.5	Sediment load	Das (1968)
Sapta Kosi River	1.0	Sediment load	Das (1968)
Kosi River	1.0	Suspended sediment load	Schumm (1963)
Sun River	1.4	Sediment load	Das (1968)
Marsyandi River	1.5–2	Detrital thermochronometry	Brewer (2001)
Tamar River basin	2.6	Sediment load	Das (1968)
High Himalayan basins	2.7±0.3	<sup>10</sup> Be and <sup>26</sup> Al on river sands	Vance et al. (2003)
Sutlej High Himalaya	1.1–1.4	Apatite fission track	Thiede et al. (2004)
Garhwal High Himalaya	2	Apatite fission track	Sorkhabi et al. (1996)
<i>Local incision rates along major rivers</i>			
Arun	1–8	<sup>14</sup> C dating of terraces	Lavé and Avouac (2001)
Arun	4–8	Calibrated incision model	Lavé and Avouac (2001)
Marsyandi	5–10	Calibrated incision model	Lavé and Avouac (2001)
Marsyandi	1.5–7	<sup>10</sup> Be and <sup>26</sup> Al on terraces	Pratt-Situala et al. (2004)
Indus	2–12	<sup>10</sup> Be and <sup>26</sup> Al on terraces	Burbank et al. (1996)
Indus	22±11	–	Shroder and Bishop (2000)
Sutlej	3.1–4.8	Zircon–apatite fission track	Jain et al. (2000)
Tsangpo	10	Zircon fission track, U–Pb	Burg et al. (1997)
Bagmati and Bakeya	15	<sup>14</sup> C dating of terraces	Lavé and Avouac (2000)



magnitude higher than average rates for the range as a whole. Based on geothermobarometric data and restored cross-sections, [Einsele et al. \(1996\)](#) reported an average denudation rate for the High Himalaya of  $1 \text{ mm year}^{-1}$  for the past 20 Ma. [Galy and France-Lanord \(2001\)](#) reported whole-basin erosion rates across the Himalaya ranged from 2.1 to 2.9  $\text{mm year}^{-1}$ . Similarly, [Vance et al. \(2003\)](#) reported whole catchment erosion rates of  $2.7 \pm 0.3 \text{ mm year}^{-1}$  for High Himalaya drainage basins based on cosmogenic isotope inventories of river sediments. In contrast, [Burbank et al. \(1996\)](#) reported local river incision rates of 2 to 12  $\text{mm year}^{-1}$  along the gorge of the Indus River. [Shroder and Bishop \(2000\)](#) reported river incision rates of  $22 \pm 11 \text{ mm year}^{-1}$  along the Indus River in the vicinity of Nanga Parbat. [Pratt-Situala et al. \(2004\)](#) reported incision rates along the Marsyandi River of up to  $7 \text{ mm year}^{-1}$  in the High Himalaya. [Burg et al. \(1997\)](#) reported mineral cooling ages that indicated exhumation sustained over millions of years at rates of  $10 \text{ mm year}^{-1}$  in the area centered around the gorge of the Tsangpo River. Consequently, there is the potential for substantial gradients in far-field to near-field rock uplift rates in response to differences in bedrock erosion rate between the gorges of major Himalayan rivers and the surrounding areas of the range.

Available data on the spatial pattern of exhumation rates in the drainage basin of the Sutlej River further suggest the potential for sustained spatial gradients in rock uplift over millions of years. [Thiede et al. \(2004\)](#) reported apatite fission track ages for two vertical transects along the high Himalayan crystalline core of  $1.1 \pm 0.4 \text{ mm year}^{-1}$  and  $1.4 \pm 0.2 \text{ mm year}^{-1}$ . While [Thiede et al. \(2004\)](#) reported the youngest cooling ages from along the Sutlej River, the sampling transect over which their reported rates were averaged covered an area that extended well away from the river and its gorge. [Jain et al. \(2000\)](#) reported exhumation rates of  $2.01 \pm 0.35 \text{ mm year}^{-1}$  to  $4.82 \pm 0.55 \text{ mm year}^{-1}$  based on fission track zircon–apatite ages for the Himalayan Metamorphic Belt from a transect through the gorge of the Sutlej River. It therefore appears that at least for the past several million years exhumation rates have been several times greater along the gorge of the Sutlej River than across the drainage basin as a whole.

The potential magnitude of the isostatic rebound and flexural response due to localized erosion depends on the flexural rigidity of the crust, which in turn depends on the effective elastic thickness of the crust. The actual thickness of continental crust is greater than its effective elastic thickness, and [Maggi et al. \(2000\)](#) argued that the

effective elastic thickness of the crust is generally less than the seismogenic thickness. Based on this reasoning and the observed depth of crustal earthquakes, [Maggi et al. \(2000\)](#) concluded that the effective elastic thickness of continental crust is generally between 10 and 40 km, which is equivalent to a flexural rigidity of  $10^{21}$  to  $10^{23} \text{ N m}$ . Based on their analysis of earthquake depths, [Maggi et al. \(2000\)](#) further argued that the effective elastic thickness for the Himalayan forelands was about 37 km, roughly double the thickness of the seismogenic zone beneath Tibet. [Masek et al. \(1994\)](#) analyzed the flexural rebound across fault-bounded grabens on the Tibetan Plateau and found that the 30–40 km wavelengths for local uplift on rift-flank margins implied flexural rigidity of  $2\text{--}6 \times 10^{20} \text{ N m}$ . Consequently, flexural rigidity of  $10^{20}$  to  $10^{23} \text{ N m}$  span the range of reasonable estimates for the flexural rigidity of the crust beneath Himalayan rivers. Even if simple isostatic rebound is not the primary mechanism responsible for forming Himalayan river anticlines, flexural rigidity of the crust should scale the extent of the zone across which rock uplift occurs in response to locally concentrated erosion. Hence, the wavelength of Himalayan river anticlines may be influenced by flexural length scales even if the process is not simple isostatic rebound.

The amplitude of a river anticline formed by isostatic response to differential erosion is more difficult to estimate than is the wavelength because of uncertainty in the total amount of material removed since the start of the Himalayan orogeny. For the case where isostatic uplift replaces half the eroded material, a difference in near-river versus far-field erosion rate of just  $2 \text{ mm year}^{-1}$  sustained over 10 Myr could produce the 10 km structural relief of Himalayan river anticlines. Such a difference in near and far field erosion rates is within the range of the available data ([Table 1](#)), and development of 10 km of structural relief since 20 Ma is possible given that  $\approx 20 \text{ km}$  of material has been removed from the High Himalaya over that time period ([Sorkhabi and Stump, 1993](#)). Another potential contributing factor to the development of river anticlines is the localization of compression along zones of thermal weakening due to rapid exhumation along steep reaches of the largest trans-Himalayan rivers. [Simpson \(2004\)](#) describes how river incision in a compressional environment can cause larger anticlines to develop than one would expect from simple flexural response to localized unloading. While the Himalayan syntaxes represent zones of localized arc-parallel compression ([Seeber and Pêcher, 1998](#)), the presence of numerous transverse extensional grabens

along the Himalaya and Tibetan Plateau (Masek et al., 1994) indicates recent range-parallel extension. If along-range extension characterizes recent deformation in the Himalaya, then it is difficult to justify range-parallel compression as an explanation for the development of late-stage, transverse river anticlines. Instead this points to the rivers themselves acting as local foci for bedrock incision and focused exhumation.

Zeitler et al. (2001) proposed that the rapid focused bedrock incision in the gorge of the Tsangpo River led to a thermal weakening of the crust, localized exhumation and upward advection of rock sustained at rates up to  $10 \text{ mm year}^{-1}$ . They proposed that rapid river incision led to the development of positive feedback and a “tectonic aneurysm” that sustained gradients in bedrock erosion between the area of the gorge and the surrounding mountains. In a numerical model of crustal convergence and erosion across the convergent plate margin of the Indo–Eurasian collision, Beaumont et al. (2001) showed how low-viscosity crustal channels coupled to zones of focused surface denudation could account for many large-scale features produced by Himalayan tectonics. Perhaps Himalayan river anticlines provide less dramatic, finer-scale examples of such feedback between tectonic and erosional processes involving crustal weakening and channeling of crustal flow. If so, the development of Himalayan river anticlines appears to be a case where rivers not only occupy structural highs but contribute to their development in locations where tectonic processes are capable of sustaining the elevation, and slopes, of even highly erosive rivers over geologic time.

The general spatial coincidence of zones of high rainfall and areas where rocks of the Lesser Himalayan sequence are exposed in structural windows are also noted. Analogous to the findings of Reiners et al. (2003) in the Cascade Range, concentration of erosion in these areas of higher than average precipitation on the flank of the range may be responsible for sustained gradients in

exhumation and thereby formation of local geological structures. Moreover, it is intriguing to suggest that advection of monsoon precipitation up major valleys contributed to enhanced exhumation along major river valleys. Viewed from this perspective, the low EI values along the Arun River south of  $27.5^\circ \text{ N}$  suggest northward migration of the locus of high erosion rates over the past 20 Ma. Einsele et al. (1996) concluded that the southern slope of the High Himalaya retreated by about 70 km over the past 20 Myr and it is intriguing to consider the possibility that the Arun River anticline reflects the transient migration of a zone of enhanced erosion tracking the retreat of the Himalayan front.

The style of feature that develops in a particular structural and geomorphic setting may reflect both the size of the river and crustal strength, with a continuum of features from transverse anticlines for smaller rivers and stronger crust, to river-parallel anticlines and ultimately (or perhaps eventually as the case may be) into tectonic aneurysms where large highly erosive rivers carve into locally weakened crust (Fig. 5). The case of transverse anticlines explored by Simpson (2004) may represent features typical of a strong crust case, and the small response that he predicted highlights the importance of crustal strength in determining the structural expression of bedrock river incision. River anticlines such as those described along many Himalayan rivers likely represent interaction of large, highly erosive rivers and relatively weak crust, with tectonic aneurysms representing the extreme case. While models for all of these cases assume that tectonic processes keep pace with erosion, recent studies (Beaumont et al., 2001; Koons et al., 2002) have shown how focused erosion can lead to and/or support channeled crustal flow that allows such a balance to be sustained. In this sense, Himalayan river anticlines may represent the surface expression or extension of relatively fine-scale crustal channels due, at least in part, to spatial variability in erosion rates.

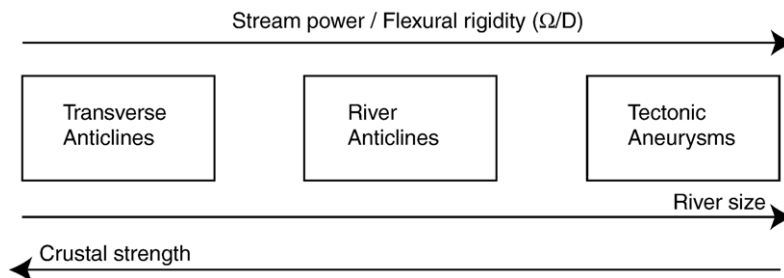


Fig. 5. Schematic illustration of hypothesized controls on the range in the styles of linkages between bedrock river erosion and the development of geological structures.

## 7. Conclusions

The growth and development of Himalayan river anticlines are not explained well by classical explanations for relationships between river courses and geological structure. Re-examination of the potential role of differential bedrock erosion suggests that rivers appear able to influence the development of geological structures where there are sustained gradients in erosion rate and either a crustal rigidity low enough to permit localized isostatic rebound, or where facilitated by active feedback between tectonic and erosional processes such as that leading to channeling of crustal flow. Consequently, rivers may be the authors not only of their own valleys, but in some circumstances the structural geology of the surrounding mountains as well.

## Acknowledgements

This work was supported in part by the National Science Foundation Continental Dynamics Program (EAR-0003561). We thank Greg Balco for bringing the salt domes along the Colorado River to our attention, Bernard Hallet for stimulating discussions of Himalayan erosion, and Alison Anders for influencing our thinking about the role of spatial variability in precipitation on erosion in the Himalaya.

## References

- Alvarez, W., 1999. Drainage on evolving fold-thrust belts: a study of transverse canyons in the Apennines. *Basin Research* 11, 267–284.
- Anders, A.M., Roe, G.H., Hallet, B., Montgomery, D.R., Finnegan, N. J., Putkonen, J., 2006. Spatial patterns of precipitation and topography in the Himalaya. In: Willett, S.D., Hovius, N., Brandon, M.T., Fisher, D.M. (Eds.), *Tectonics, Climate and Landscape Evolution*, Special Paper 398. Geological Society of America, Boulder, pp. 39–54.
- Beaumont, C., Jamieson, R.A., Nguyen, M.H., Lee, B., 2001. Himalayan tectonics explained by extrusion of a low-viscosity crustal channel coupled to focused surface denudation. *Nature* 414, 738–742.
- Bordet, P., 1955. Les elements structuraux de l'Himalaya de l'Arun et la region de l'Everest. *Comptes Rendus de l'Académie des Sciences* 240, 102–104.
- Brewer, I.D., 2001. Detrital-mineral thermochronology: investigations of orogenic denudation in the Himalaya of central Nepal. Ph.D. Dissertation, Pennsylvania State University, State College. 181 pp.
- Burbank, D.W., Leland, J., Fielding, E., Anderson, R.S., Brozovic, N., Reid, M.R., Duncan, C., 1996. Bedrock incision, rock uplift and threshold hillslopes in the northwestern Himalayas. *Nature* 379, 505–510.
- Burbank, D.W., McLean, J.K., Bullen, M., Abdрахmatov, K.Y., Miller, M.M., 1999. Partitioning of intermontane basins by thrust-related folding, Tien Shan, Kyrgyzstan. *Basin Research* 11, 75–92.
- Burg, J.-P., Davy, P., Nievergelt, P., Oberli, F., Seward, D., Diao, Z., Meier, M., 1997. Exhumation during crustal folding in the Namche-Barwa syntaxis. *Terra Nova* 9, 53–56.
- Das, S.K.N., 1968. Soil erosion and the problem of silting in the Kosi catchment. *Journal of Soil and Water Conservation in India* 16 (3–4), 60–67.
- DiPietro, J.A., Pogue, K.R., Hussain, A., Ahmad, I., 1999. Geologic map of the Indus syntaxis and surrounding area, northwest Himalaya, Pakistan. In: Macfarlane, A., Sorkhabi, R.B., Quade, J. (Eds.), *Himalaya and Tibet: Mountain Roots to Mountain Tops*. Geological Society of America Special Paper, vol. 328. Geological Society of America, Boulder, pp. 159–178.
- Einsele, G., Ratschbacher, L., Wetzel, A., 1996. The Himalaya–Bengal Fan denudation–accumulation system during the past 20 Ma. *Journal of Geology* 104, 163–184.
- Finlayson, D., Montgomery, D.R., Hallet, B.H., 2002. Spatial coincidence of rapid inferred erosion with young metamorphic massifs in the Himalayas. *Geology* 30, 219–222.
- Finnegan, N.J., Roe, G., Montgomery, D.R., Hallet, B., 2005. A scaling relationship for channel width in bedrock rivers. *Geology* 33, 229–232.
- Galy, A., France-Lanord, C., 2001. Higher erosion rates in the Himalaya: geochemical constraints on riverine fluxes. *Geology* 29, 23–26.
- Gansser, A., 1964. *Geology of the Himalaya*. Wiley-Interscience, New York.
- Harrison, T.S., 1927. Colorado–Utah salt domes. *Bulletin of the American Association of Petroleum Geologists* 11, 111–133.
- Hetenyi, H., 1946. *Beams on Plastic Foundation*. University of Michigan Press, Ann Arbor.
- Huntoon, P.W., Elston, D.P., 1979. Origin of the River Anticlines, Central Grand Canyon, Arizona, U.S. Geological Survey Professional Paper, vol. 1126-A. U.S. Government Printing Office, Washington, D. C.
- Jain, A.K., Kumar, D., Singh, S., Kuman, A., Lal, N., 2000. Timing, quantification and tectonic modeling of Pliocene–Quaternary movements in the NW Himalaya: evidence from fission track dating. *Earth and Planetary Science Letters* 179, 437–451.
- Koons, P.O., Zeitler, P.K., Chamberlain, C.P., Craw, D., Meltzer, A.S., 2002. Mechanical links between erosion and metamorphism in Nanga Parbat, Pakistan Himalaya. *American Journal of Science* 302, 749–773.
- Krishnaswamy, V.S., 1981. Status report of the work carried out by the Geological Survey of India in the framework of the International Geodynamics Project. In: Gupta, H.K., Delany, F.M. (Eds.), *Zagros-Hindu Kush-Himalaya Geodynamic Evolution*. American Geophysical Union, Washington, D.C., pp. 169–188.
- Lavé, J., Avouac, J.P., 2000. Active folding of fluvial terraces across the Siwaliks Hills, Himalayas of central Nepal. *Journal of Geophysical Research* 105, 5735–5770.
- Lavé, J., Avouac, J.P., 2001. Fluvial incision and tectonic uplift across the Himalayas of central Nepal. *Journal of Geophysical Research* 106, 26,561–26,591.
- Maggi, A., Jackson, J.A., McKenzie, D., Priestley, K., 2000. Earthquake focal depths, effective elastic thickness, and the strength of the continental lithosphere. *Geology* 28, 495–498.
- Masek, J.G., Isacks, B.L., Fielding, E.J., 1994. Rift flank uplift in Tibet: evidence for a viscous lower crust. *Tectonics* 13, 659–667.
- Meier, K., Hiltner, E., 1993. Deformation and metamorphism within the Main Central Thrust zone, Arun Tectonic Window, eastern Nepal. In: Treloar, P.J., Searle, M.P. (Eds.), *Himalayan Tectonics*.

- Geological Society Special Publication, vol. 74. The Geological Society, London, pp. 511–523.
- Montgomery, D.R., 1994. Valley incision and the uplift of mountain peaks. *Journal of Geophysical Research* 99, 13,913–13,921.
- Montgomery, D.R., 2001. Slope distributions, threshold hillslopes and steady-state topography. *American Journal of Science* 301, 432–454.
- Norris, R.J., Cooper, A.F., 1997. Erosional control on the structural evolution of a transpressional thrust complex on the Alpine Fault, New Zealand. *Journal of Structural Geology* 19, 1323–1342.
- Oberlander, T.M., 1965. The Zagros Streams. Syracuse University Geographical Series, vol. 1.
- Oberlander, T.M., 1985. Origin of drainage transverse to structures in orogens. In: Morisawa, M., Hack, J.T. (Eds.), *Tectonic Geomorphology*. Allen and Unwin, Boston, pp. 155–182.
- Pavlis, T.L., Hamburger, M.W., Pavlis, G.L., 1997. Erosional processes as a control on the structural evolution of an actively deforming fold and thrust belt: an example from the Pamir-Tien Shan region, central Asia. *Tectonics* 16, 810–822.
- Powell, J.W., 1875. *Exploration of the Colorado River of the West and its Tributaries*. Government Printing Office, Washington, D. C.
- Pratt-Situala, B., Burbank, D.W., Heimsath, A., Ojha, T., 2004. Landscape disequilibrium on 1000–10,000 year scales Marsyandi River, Nepal, central Himalaya. *Geomorphology* 58, 223–241.
- Reiners, P.W., Ehlers, T.A., Mitchell, S.G., Montgomery, D.R., 2003. Coupled spatial variations in precipitation and long-term erosion rates across the Washington Cascades. *Nature* 426, 645–647.
- Seeber, L., Pêcher, A., 1998. Strain partitioning along the Himalayan arc and the Nanga Parbat antiform. *Geology* 26, 791–794.
- Schelling, D., 1992. The tectonostratigraphy and structure of the eastern Nepal Himalaya. *Tectonics* 11, 925–943.
- Shroder Jr., J.F., Bishop, M.P., 2000. Unroofing of the Nanga Parbat Himalaya, in *Tectonics of the Nanga Parbat Syntaxis and the Western Himalaya*. In: Khan, M.A., Treloar, P.J., Searle, M.P., Jan, M.Q. (Eds.), Geological Society, London Special Publication, vol. 170, pp. 163–179.
- Schumm, S.A., 1963. The disparity between present rates of denudation and orogeny. U.S. Geological Survey Professional Paper, vol. 454-H. United States Government Printing Office, Washington, D.C.
- Simpson, G., 2004. Role of river incision in enhancing deformation. *Geology* 32, 341–344.
- Sorkhabi, R. B., and Stump, E., 1993. Rise of the Himalaya: a geochronologic approach, *GSA Today*, v. 3(4), p. 85, 88–92.
- Sorkhabi, R.B., Stump, E., Foland, K.A., Jain, A.K., 1996. Fission-track and  $^{40}\text{Ar}/^{39}\text{Ar}$  evidence for episodic denudation of the Gangotri granites in the Garhwal Higher Himalaya, India. *Tectonophysics* 260, 187–199.
- Thiede, R.C., Bookhage, B., Arrowsmith, J.R., Sobel, E.R., Strecker, M.R., 2004. Climatic control on rapid exhumation along the Southern Himalayan Front. *Earth and Planetary Science Letters* 222, 791–806.
- Tucker, G.E., Slingerland, R.L., 1994. Erosional dynamics, flexural isostasy, and long-lived escarpments: a numerical modeling study. *Journal of Geophysical Research* 99, 12,229–12,243.
- Vance, D., Bickle, M., Ivy-Ochs, S., Kubik, P.W., 2003. Erosion and exhumation in the Himalaya from cosmogenic isotope inventories of river sediments. *Earth and Planetary Science Letters* 206, 273–288.
- Wager, L.R., 1937. The Arun river drainage pattern and the rise of the Himalaya. *Geographical Journal* 89, 239–250.
- Zeitler, P.K., et al., 2001. Erosion, Himalayan geodynamics, and the geomorphology of metamorphism. *GSA Today* 11, 4–9.